Combined real time Ultrasound-thermometry and Elastography imaging during HIFU therapy: ex-vivo results

Bastien Arnal, Mathieu Pernot, Mickael Tanter

10ème Congrès Français d'Acoustique
Lyon, 12-16 Avril 2010

Combined real time Ultrasound-thermometry and Elastography imaging during HIFU therapy: ex-vivo results

Bastien Arnal[1], Mathieu Pernot[1], Mickael Tanter[1]

[1]Institut Langevin Ondes et Images, ESPCI, 10 rue Vauquelin 75005 Paris, FRANCE

The use of High intensity Focused Ultrasound (HIFU) for non invasive therapy requires improving real-time monitoring of the lesion formation during treatment, to avoid damage of the surrounding healthy tissues. The goal of this study is to show the feasibility of a full ultrasound approach that relies on the assessment of the changes in both tissue elasticity and temperature implemented on conventional ultrasonic imaging probes. HIFU treatment and monitoring were performed using a confocal set made up of a 8MHz ultrasound diagnostic probe (Vermon) and a 2.5MHz single element transducer focused at 30mm (Imasonic) on ex-vivo porcine samples. 2D temperature estimation was combined with Supersonic Shear Imaging (SSI) on the same device (Aixplorer, SuperSonic Imagine). To lower the thermo-acoustic lens effect, the ultrasound thermometry was performed using plane wave emissions steered at 13 angles (+/-12 degrees). The SSI sequence consisted in 2 successive shear waves induced at different lateral positions. Each wave was created thanks to pushing beams of 100µs at 3 depths. The shear wave propagation was acquired at 17000 frames/s, from which the elasticity map was recovered. HIFU sonications were interleaved with fast imaging acquisitions allowing a duty cycle of more than 90%. Elasticity and temperature mapping was achieved every 5 seconds during treatment. Tissue stiffness was found to decrease at the focal zone with temperature up to 50°C. Ultrasound-based temperature estimation was highly-correlated to stiffness variation maps. The lesion formation comes with a strong increase (up to four-fold) of the elastic modulus. These combined methods provide complementary measurements of tissue properties and overcome the limitations of US-thermometry alone as SSI acquisitions are motion-insensitive. A full ultrasound-based monitoring technique was developed to achieve elasticity and temperature mapping of soft tissues under HIFU treatment. It demonstrated the feasibility of monitoring and detecting the HIFU thermal lesion.

1 Introduction

High Intensity Focused Ultrasound (HIFU) is now a validated therapeutic technique for the treatment of tumours in a broad variety of organs such as the liver (ter Haar *et al*. 1989; Wang *et al*. 2003), the prostate (Chapelon *et al*. 1992b; Foster *et al.* 1993; Chapelon *et al*. 1999a), the kidney (Chapelon *et al*. 1992A; Hynynen *et al*. 1995; Damianou 2003), the brain (Fry *et al.* 1954; Vykhodtseva *et al.* 1994) and the breast (Wu *et al*. 2003). These types of treatments require that the treated region be controlled and monitored in order to avoid damaging of surrounding healthy tissue.

Magnetic Resonance Imaging (MRI) provides quasi real-time three dimensional temperature maps with a very good localization of the heated region, but is costly and complex to use. In contrast, fully ultrasound-based method could be easily integrated into HIFU systems with relatively low cost and a high portability.

One one hand, the feasibility of temperature estimation during HIFU therapy using pulse-echo diagnostic ultrasound data has been demonstrated by Seip *et al.* [1] . This method can be applied for two-dimensional (2D) real-time non-invasive temperature estimation using diagnostic ultrasound. This technique is based on tracking the shifts in the backscattered RF signals (ie., speckle) due to thermal expansion and local change in the speed of sound.

However, ultrasound thermometry has not ever been used for in-vivo applications as this method has some limitations. First, the echo-strain estimations can be wrong due to cardiac-induced or respiratory movements. Second, he temperature dependence of echo-strain varies strongly between tissues. Although this coefficient can be experimentally determined for different tissues, it remains unknown in heterogeneous tissues such as breast. R. Miller *et al.* have shown that this law varies a lot depending on the fat content in liver samples [3]. In most of the tissues, this temperature dependence makes the estimation above 45-50°C impossible due to the temperature dependence of the speed of sound and due to thermal expansion. Nevertheless, Souchon *et al.* have shown the feasibility to monitor the formation of thermal lesions via echo-strain imaging [4], thanks to significant and exploitable thermal expansion in the lesion area.

On the other hand, elastography has been extensively investigated for the characterization of HIFU-induced lesions. In 1998, the use of static elastography to visualise thermal-lesions was first investigated *in vitro* by Stafford *et al.* [5], then by Kallel *et al.* [6] in the rabbit paraspinal skeletal muscle and by Righetti *et al.* [7] in canine liver. In-vivo test were reported by Varghese *et al*.[8] on pig liver and Souchon *et al*. [9] on human prostate. Dynamic elastography techniques have also been investigated. Magnetic resonance elastography (MRE) and dynamic elastometry rely on monochromatic excitations. MRE has been proven to be robust but has the inconveniences of MRI. Acoustic-radiation-force-based approaches have also been under investigation [10], [11] but these techniques

have a high exposure time to the radiation force pushing sequence and are intrinsically not quantitative.

Bercoff *et al*. proposed to use the supersonic shear imaging technique (SSI) [12], to monitor elasticity during HIFU treatment before and after the necrosis threshold [13]. Recent clinical studies show the reliability of this technique to map the elasticity of soft tissues [14],[15].

Moreover, recent ex-vivo studies by Sapin-de Brosses *et al*. [16], using SSI show the feasibility of monitoring the changes of stiffness linked to a temperature elevation.

Here, we propose to use SSI during HIFU treatment to access to the dynamics of the bio-mechanical properties in real-time. The study is done in-vitro in gelatine and on porcine muscle ex-vivo samples. On all of this materials, the shear modulus is shown to decrease with temperature in the heated region below the necrosis threshold. On bio-tissues samples, the necrosis shows a strong increase of the shear modulus observable either in short-time or long-time measurements depending on the HIFU acoustic power.

Thus, Shear wave and US-thermometry can be combined to overcome US-thermometry limitations and to perform a valid monitoring until the end of the treatment. The high-resolution of US-thermometry allows to position the heated region. Indeed, the variance of Shear modulus maps and the lower sensitivity and resolution of the technique do not allow this. Still, US-thermometry is used to quantify temperatures up to 45°C. Shear modulus values can be calibrated with temperature estimations and stay valid at any time. Finally, this paper demonstrates the feasibility of doing Shear-Wave thermometry. This technique is motion-insensitive and displays a very good parameter to access to the necrosis threshold in real-time with a good resolution.

2 Material and methods

2.1 Two-dimensional Temperature (strain-maps) estimation using compound imaging.

Ultrasonic temperature estimation is based upon the thermal dependence of the backscattered signal [1]. Two physical phenomena are involved in the modification of the speckle during heating: the temperature dependence of the speed of sound and the thermal expansion. According to Simon *et al.* [2], the temperature elevation along the beam axis can be related to the axial displacement:

$$\Delta T = \frac{c_0}{2(\alpha-\beta)}\frac{\partial \delta t}{\partial z}$$

where δt is the estimated time-shift at position (x,z), c_0 is the initial speed of sound in the medium, a is the linear coefficient of thermal expansion, and the coefficient $\beta=1/c_0\ \delta c/\delta T$ related the change in the speed of sound with temperature. In this model, it is assumed that the parameter $k=1/(\alpha-\beta)$ is a constant. The temperature echo-shift dependence is then supposed linear over a limited range of temperature elevation, typically up to 45-50°C.

The time-shift occurring between two successive images is estimated using a new speckle tracking technique. An in phase/quadrature (IQ) modulation is performed on the RF raw data. The cross-correlation between IQ_1 and IQ_2 is calculated over small overlapping data window of $\Delta z=8\lambda$. We use a monochromatic approach:

$$C(x,z) = \int_{z}^{z+\Delta z} IQ_1(x,z)\,IQ_2(x,z)^*\,dz$$

assuming that: $IQ_2(x_0,z_0) = IQ_1(x_0,z_0).e^{2\pi.f.\tau}$

The echo-shift is then: $\tau(x,z) = \frac{1}{2\pi.f}Arg(C(x,z))$

This method is computationally efficient and is able to be implemented in real-time for motion-tracking with an accurate estimation of small time-shifts (~5ns). Once the time-shifts map is estimated, the temperature map is computed by differentiating the time-shift along the beam axis **k**.

However, the thermo-lens effect created by sharp lateral gradients in the temperature distribution can lead to artifacts in the estimation. Pernot *et al.* [17] have recently proposed an elegant method based on spatial compound imaging. This approach consists in imaging the media using steered plane wave. A 2D temperature map is estimated from axial displacement maps between consecutive RF images of identically steered plane wave insonification. Temperature estimation is improved by averaging the estimations from the multiple steered plane wave insonifications. In-vitro and ex-vivo results show a reduction in the thermal-lens effect. We will use this method for temperature-strain maps estimations.

The temperature estimation is then averaged with a spatial angular compound imaging technique, using steered plane wave at 13 angles from -12° to 12° and no sub-aperture emissions. Each map of echo-shift is filtered in the two dimensions using 1D FIR-filters designed by the Remez algorithm. The typical resolution of the final images is 2mm along the lateral dimension and 4mm along the axial dimension.

As shown by Souchon *et al.* [4], the temperature estimation can be used for imaging the deformation (strain imaging). The expression of strain s(z) is approximately:

$$s(z) = \frac{c_0}{2}\frac{\partial \tau(z)}{\partial z} \simeq \varepsilon(z) - \frac{\delta c(z)}{c_0}$$

where $\tau(z)$ is the same time-shift than defined previously. The strain-maps will be expressed in equivalent of Celsius degrees but have not to be considered as temperature estimation above 40°C.

2.2 High-resolution elastography using Supersonic Shear imaging.

SSI technique is able to provide quantitative shear modulus mapping of an organ in less than 30ms. SSI relies on the generation of a shear wave by the acoustic radiation force induced by an ultrasonic beam. To create quasi-plane shear waves with a strong amplitude, the shear source is moved at different depths created a Mach cone. Two quasi-plane shear waves propagates in opposite directions.

The propagation of this shear wave is then imaged using ultrafast imaging technique implemented on the ultrafast ultrasonic scanner Aixplorer developed by Supersonic Imagine (Aix en Provence, France). Each wave was created thanks to pushing beams of 100µs at 3 depths. The shear wave propagation was acquired at 17000 frames/s. The elasticity map is calculated using a simple time-of-flight technique that computes the value of the shear-wave speed on each point of the image. The result can be displayed either in terms of shear wave speed V_g or in terms of shear modulus $\mu=\rho V_g^2$. Here, results will be presented in shear wave speed.

To compare shear wave speed maps before and while heating, a normalization technique is needed. Sapin-de Brosses *et al*. normalized their results considering a ratio between the mean initial shear modulus and the mean current one over a large region of interest. This allowed to study various samples with different initial elasticity and compare them. This normalization method can not been applied to quantify locally a temperature effect: the effect would be underestimated for stiff regions or overestimated for soft regions. To investigate the technique, a general normalization is a differential one. Hence, results will be presented in shear wave speed difference in m/s:

$$\Delta Vg(t,T)=Vg(t,T)-Vg(t=0,T_0)$$

where Vg(t,T) is the group velocity of the shear wave at the time t of treatment.

2.3 Experimental setup.

HIFU treatment and monitoring was performed using a confocal set made up of a 8MHz ultrasound diagnostic probe (Vermon) and a 2.5MHz single element transducer focused at 34mm (f/D=1, Imasonic) (see Figure 1). This setup was designed for in-vivo experimental conditions as the whole system can be placed directly on the skin. The contact between the HIFU transducer and the bound of the sample is ensured by a fixed water balloon made in latex.

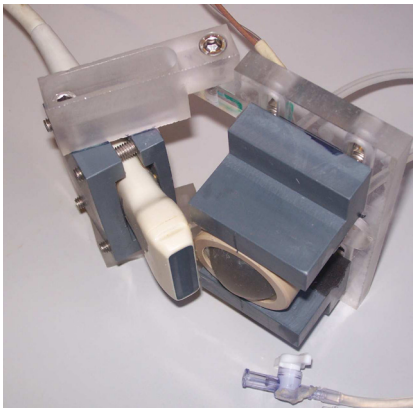

Figure 1 : Confocal set for HIFU treatment and monitoring.

HIFU sonications were interleaved with fast imaging acquisitions allowing a duty cycle of more than 80%. Each acquisitions consisted in a B-mode image, a sequence designed for thermometry and a sequence designed for shear wave imaging. Elasticity and temperature mapping were achieved every 5 seconds during treatment. Only temperature maps are displayed in real-time and elasticity maps are processed off-line.

2.4 In-vitro and ex-vivo samples.

A preliminary study has been done in-vitro on a gelatine phantom (8% + cellulose 2%).

Previous studies of the dependence of elasticity with temperature were performed in bovine muscle [16]. Presented results will be on porcine muscle (24h after procurement).

3 Results

3.1 In vitro evaluation of the Shear-wave imaging technique.

Experiments were initially performed on gelatine phantoms to prove the feasibility of imaging the small inclusion created during the treatment. The phantom shear speed is quite homogeneous: 1,11 +/- 0,07m/s. . The results is displayed in Shear-speed difference (m/s) between the initial map and the current map, every 5 seconds during the treatment. An example is shown after 45 seconds of treatment.

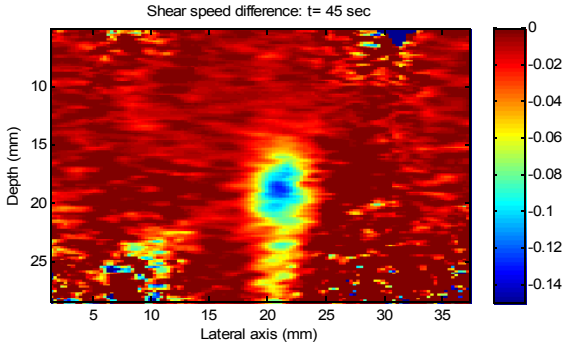

Figure 2 : Shear speed difference (m/s) after 45sec of treatment.

The typical size of the heated region is 5mm along depth and 4,5mm along lateral axis. The shear speed difference at this time outside the treated area was not significant. To illustrate the dynamics of evolution of the shear speed difference, some random points are picked and the following graph can be displayed:

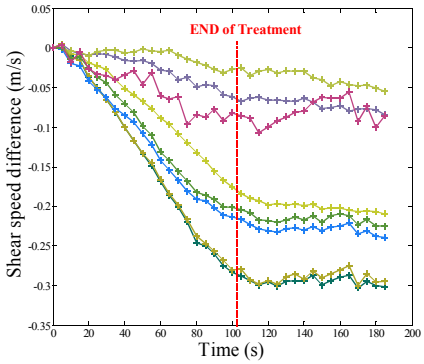

Figure 3 : Shear speed difference evolution during the treatment.

The maximum amplitude of shear speed variation is around 0.3m/s which correspond to 27% of the initial speed. The sensitivity of the speed evaluation is estimated at best of 0.01m/s which correspond to a sensitivity of 2°C for the pork muscle as shown in the next part.. To ensure the right position of the focus compared to the maximum of the elasticity variation, a temperature-strain map can be superimposed.

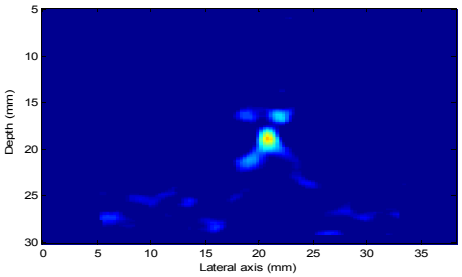

Figure 4 : Strain-imaging map after 45sec of treatment.

This results illustrates that the heated region is well localized thanks to the differential shear wave imaging technique. The quantitative aspect is discussed in the next part.

3.2 Ex vivo results: low temperature elevation (below 43°)

For reasonable temperature elevations, US-thermometry has been validated to quantify temperature with a low variance (less than 1°C). Sapin-de Brosses *et al.* established shear-modulus temperature dependence using a thermally controlled bath as a mean of heating [16]. In this study the normalized shear modulus (in %) was found to decrease of -2.0%/°C between 37°C and 43°C).

Here, a porcine muscle sample is placed in a thermally controlled water tank at a fixed temperature (30°C). The HIFU treatment is applied during 110s with an acoustic power of Pac=3,75W. The initial shear speed value in the ROI was 2,46m/s +/-0,16. The Figure 4 shows curves from a local region of interest where shear speed evaluation can be trusted.

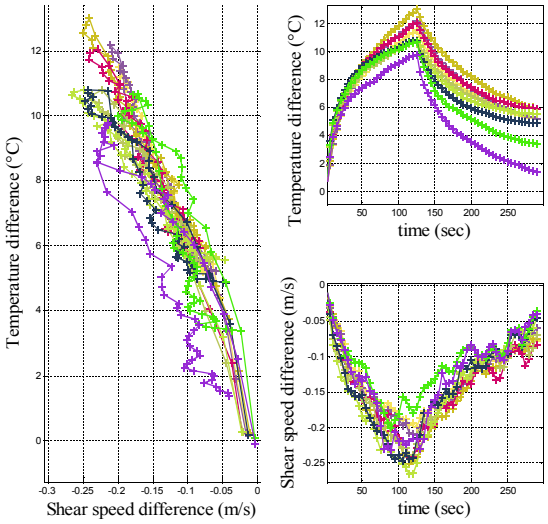

Figure 4 : Shear wave speed difference and Temperature elevation correlation.

As previously found in bovine muscle, the shear modulus was found to decrease with temperature. The mean slope of the Shear speed difference temperature dependence is around -0,3m/s/°C. The results in terms of normalized shear modulus gives a rate equal to -2,1%/°C. This is close to Sapin-de Brosses's values and demonstrate the quantitative consistence of this method, even comparing muscles from different species. Moreover, as shown on Figure. 4, a good correlation was found between the shear modulus and the echo-strain temperature estimates (correlation coefficient: 0,91-0,97). Hence, this demonstrates the feasibility of quantitative shear-wave thermometry up to 43°C.

The reversibility of the transformation during heating and cooling cycle is well shown by Figure 4. This allows performing a low-temperature elevation (~+10°C) and then observe the relaxation to locally calibrate the tissue. Then, the treatment could be performed with access to the temperature using shear wave imaging. It opens a wide range of possibilities to overcome the limitations of US-thermometry.

3.3 Real-time necrosis imaging: ex-vivo results.

For higher temperature elevations, the necrosis threshold was reached and the echo-strain temperature estimation failed due to the thermal dilatation of the tissue. We investigated the generation of the tissue necrosis in porcine muscle appearing very early in the treatment, after 10 seconds of sonication (Pac=8,80W). On Figure 5, this change of stiffness is very clear and we can delimit the necrosis. The center of the ablated region becomes 3 times stiffer. The shear speed goes from 3.24m/s +/-0.26 up to 7m/s as shown of Figure 6.

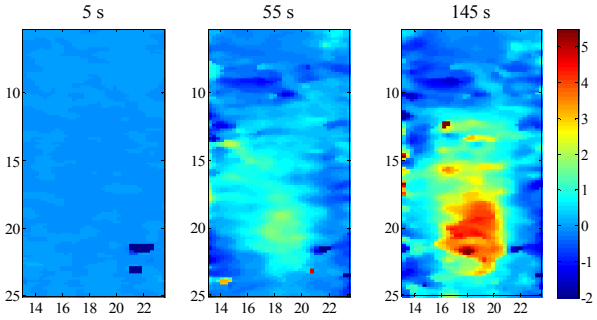

Figure 5 : Shear speed difference maps during the necrosis in porcine muscle.

The shear-speed tends to decrease in the first 10 seconds of the treatment but then explodes at 15 seconds. As shown by previous studies, this behavior is a signature of necrosis and we can even detect with a good temporal resolution its dynamics during the treatment. At the end of the treatment as the temperature decreases, the shear speed continues to increase with a different slope. This result is consistent with the previous studies of Sapin-de Brosses *et al.*[16].

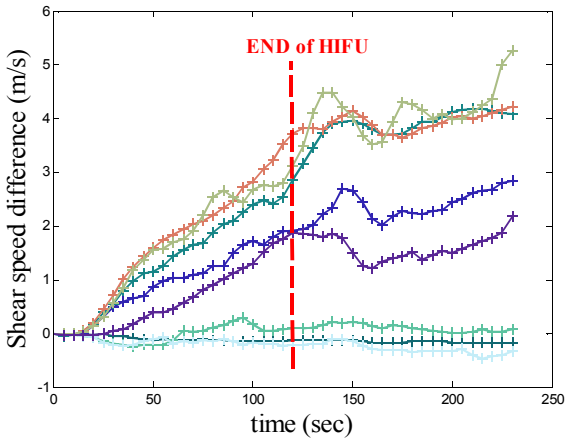

Figure 6 : Shear speed difference evolution during the necrosis in porcine muscle.

Here, shear-wave imaging can not been used to quantify temperatures. In this application, the contrast in shear-speed is very high and there is no limitations due to the variance of shear-speed maps. The size of the lesion has already been correlated with the shear wave speed maps by Bercoff *et al.* [13] with success using an optical contrast as standard. He noticed that the inversion algorithm is not true at the edges of the necrosis and lead to an underestimation of the size of the lesion of about 1mm. Here, this error is insignificant compared to the size of the lesion. Indeed, if defined at -12dB, the lesion size is estimated being of 8,2mm +/- 0,1 (axial) and 5,1mm+/-0.15 (lateral). The elliptic size of the lesion is due to the setup and due to the longer axial size of the focal spot of the HIFU transducer.

This demonstrates the feasibility of real-time control of the thermal lesion stiffness. This technique could potentially be used to stop the treatment when the targeted area has been treated.

3.4 Combined Ultrasound-thermometry and shear wave Elastography .

In many ways, we can combine these two methods to understand the evolution of the tissue while treating. During heating, three main regimes are found for the strain map technique: for low temperature elevations (up to 45°C) strain-maps are reliable for temperature estimations . Above 45°C but before thermal lesion the strain value decreases due to non linear temperature dependence of the speed of sound so that the follow-up of the temperature becomes difficult with strain maps. After thermal lesion, the change in tissue stiffness induces new strains on surrounding tissues. The thermal lesion formation is associated with a tissue compression at the center of the lesion and as a consequence, a tissue expansion surrounding the lesion [4]. This effect induces strong artifacts on the strain maps and the temperature can no longer be estimated. Liu *et al.* [18] also reported that the change of stiffness of the lesion increases the temperature echo-shift dependance for post-treatment low temperature elevations and this effect may be present in our experiment but might be relatively small compared to lesion strains. Therefore, we investigated the possibility to monitor the lesion with echo-strain imaging combined with shear wave imaging on porcine muscle. Different scenarios have been underlined and are shown on Figure 7:

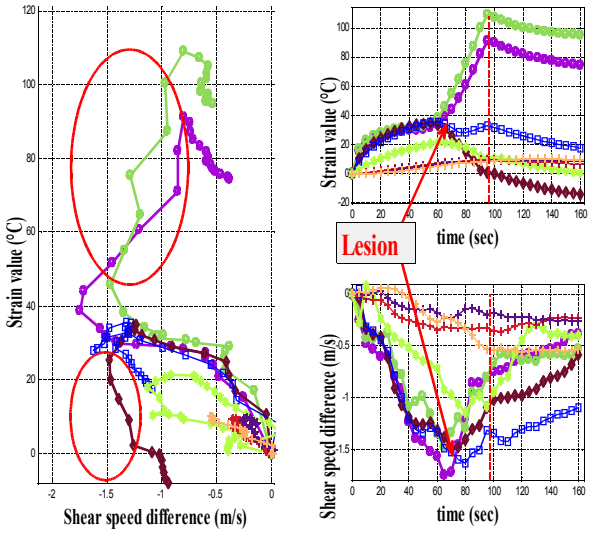

Figure 7 : Shear wave speed difference and Temperature elevation correlation.

The three previous regimes can be identified on Figure 7. First, temperature elevation is measured correctly both on strain and stiffness maps. A strong correlation is found between strain and stiffness. Secondly, Above 40°C strain maps becomes unreliable whereas stiffness continues varying with temperature. Finally, a lesion appears at 60 seconds as shown by the red arrows. The strain imaging shows a strong shrinkage . The treatment is stopped at 95 seconds. The reversible scenario is shown for curves marked with cross (+). A low temperature elevation gives no significant change in elasticity.

For higher temperature elevations, there are four different cases:

- compressional lesion giving positive strain and increase in shear wave speed before the end of the treatment (o).
- expanding lesion giving negative strain and increase in shear wave speed before the end of the treatment (brown ◊).
- compressed healthy tissue (blue □).
- expanded healthy tissue (green hexagram).

Then, it is possible to spot the lesion formation considering points appearing in the two red ellipses.

A scheme on Figure 8 presents the temperature effects and the lesion dilatation effects that would be interesting to dissociate:

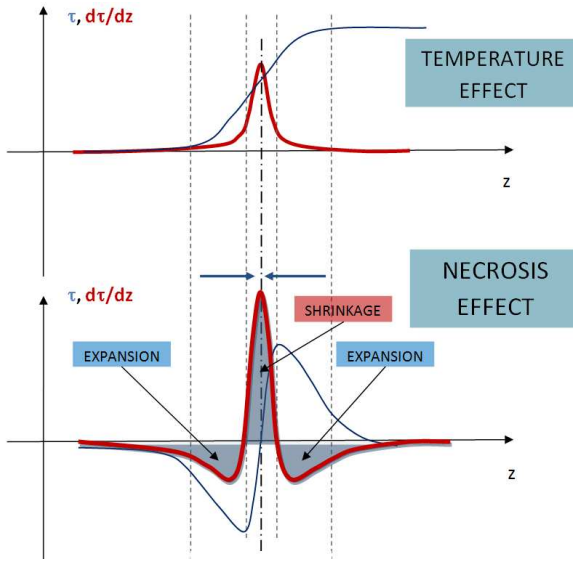

Figure 8: Time-shift (blues) and strain values (red) for the separated effects of temperature and necrosis.

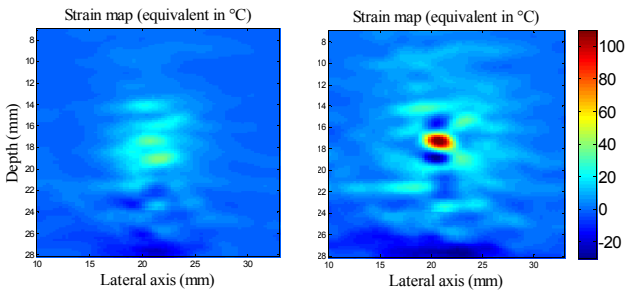

Figure 9: Strain maps before and after lesion formation.

On Figure 9, two strain maps before and after lesion are shown. High positive strain values correspond to a shrinkage and low negative values correspond to an expansion of the tissue appears. This results is in concordance with the synthesis of Figure 8. The strain-

values due to lesion formation are twice as high than the cumulative temperature at this point.

These results demonstrate that strain maps after lesion can be well interpreted using shear wave imaging maps as a critical comparison. We underline the impossibility to delimit the necrosis only using strain-maps as expanding lesion have been pointed out.

4 Conclusion

The combination of strain-imaging and shear wave elastography for monitoring the HIFU treatments is a very promising technique. It allows the recovery of bio-mecanic changes and temperature changes during heating. Experiments in gelatine confirmed the possibility of imaging 2D maps of elasticity difference. Experiments in pork muscle demonstrated the feasibility of this fully-ultrasound based technique to access the temperature evolution up to 40°C and to the necrosis evolution. After necrosis, the lesion area becomes up to 4 times stiffer. The combination of the two methods gives a good interpretation of strain imaging during necrosis. Shear wave imaging rubs out the limitations of US-thermometry as it is motion insensitive and remains a valid tool to access temperature until necrosis and dynamics of the lesion formation.

Future work will consist in validating *in-vivo* the use of this technique for HIFU treatment monitoring on sheep muscle and liver.

References

[1] R. Seip, P. VanBaren, C.A. Cain, E.S. Ebbini, "Noninvasive real-time multipoint temperature control for ultrasoundphased array treatments," *IEEE Transactions on Ultrasonics, Ferroelectrics and Frequency Control* 43, no. 6 (1996): 1063–1073.

[2] C. Simon, P. VanBaren, E. S. Ebbini, "Two-dimensional temperature estimation using diagnostic ultrasound," *IEEE Transactions on Ultrasonics, Ferroelectrics and Frequency Control* 45, no. 4 (1998): 1088–1099.

[3] N. R Miller, J. C Bamber, P. M Meaney, "Fundamental limitations of noninvasive temperature imaging by means of ultrasound echo strain estimation," *Ultrasound in medicine & biology* 28, no. 10 (2002): 1319–1333.

[4] R. Souchon, G. Bouchoux, E. Maciejko, C. Lafon D. Cathignol, M. Bertrand, J.Y Chapelon, "Monitoring the formation of thermal lesions with heat-induced echo-strain imaging: A feasibility study," *Ultrasound in medicine & biology* 31, no. 2 (2005): 251–259.

[5] R.J Stafford, F. Kallel, *et al*. "Elastographic imaging of thermal lesions in soft tissue: a preliminary study in vitro," *Ultrasound in Medicine & Biology* 24, no. 9 (Décembre 1998): 1449-1458.

[6] F. Kallel, R.J Stafford *et al*. "The feasibility of elastographic visualization of HIFU-induced thermal lesions in soft tissues," *Ultrasound in Medicine & Biology* 25, no. 4 (Mai 1999): 641-647.

[7] R. Righetti, F. Kallel, R.J Stafford *et al.* "Elastographic characterization of HIFU-induced lesions in canine livers," *Ultrasound in medicine & biology* 25, no. 7 (1999): 1099–1113.

[8] T. Varghese, J. A. Zagzebski, et F. T. Lee, "Elastographic imaging of thermal lesions in the liver in vivo following radiofrequency ablation: preliminary results," *Ultrasound in Medicine & Biology* 28, no. 11-12 (Novembre): 1467-1473.

[9] R. Souchon, O. Rouvière, A. Gelet, A. Detti, Srinivasan, J. Ophir, J.Y Chapelon, "Visualisation of HIFU lesions using elastography of the human prostate in vivo: preliminary results," *Ultrasound in Medicine & Biology* 29, no. 7 (Juillet 2003): 1007-1015.

[10] E. Konofagou, J. Thierman, et K. Hynynen, "The use of ultrasound-stimulated acoustic emission in the monitoring of modulus changes with temperature," *Ultrasonics* 41, no. 5 (Juillet 2003): 337-345.

[11] S. Girnyk, A. Barannik, E. Barannik, V. Tovstiak, A. Marusenko, V. Volokhov , "The estimation of elasticity and viscosity of soft tissues in vitro using the data of remote acoustic palpation," *Ultrasound in Medicine & Biology* 32, no. 2 (Février 2006): 211-219.

[12] J. Bercoff, M. Tanter, et M. Fink, "Supersonic shear imaging: a new technique for soft tissue elasticity mapping," *IEEE Transactions on Ultrasonics Ferroelectrics and Frequency Control* 51, no. 4 (2004): 396–409.

[13] J. Bercoff M. Pernot, M. Tanter, M. Fink, "Monitoring thermally-induced lesions with supersonic shear imaging.," *Ultrasonic imaging* 26, no. 2 (2004): 71.

[14] M. Tanter et al., "Quantitative assessment of breast lesion viscoelasticity: initial clinical results using supersonic shear imaging," *Ultrasound in Medicine & Biology* 34, no. 9 (2008): 1373–1386.

[15] M. Tanter et al., "Quantitative Assessment of Breast Lesion Viscoelasticity: Initial Clinical Results Using Supersonic Shear Imaging," *Ultrasound in Medicine & Biology* 34, no. 9 (Septembre 2008): 1373-1386.

[16] E. Sapin-de Brosses, J.L Genission, M. Pernot, M. Fink, M. Tanter, "Temperature dependence of the shear modulus of soft tissues assessed by ultrasound." Physics in Medecine & Biology 55 (2010) 1-18

[17] M. Pernot, M. Tanter, J. Bercoff, K.R Waters, "Temperature estimation using ultrasonic spatial compound imaging," *Ieee Transactions on Ultrasonics Ferroelectrics and Frequency Control* 51, no. 5 (2004): 606–615.

[18] D. Liu, E.S Ebbini, "Real-Time 2-D Temperature Imaging Using Ultrasound," *Biomedical Engineering, IEEE Transactions on* , vol.57, no.1, pp.12-16, Jan. 2010